ELSEVIER

International Journal of Mass Spectrometry 222 (2003) 135–153

International Journal of Mass Spectrometry

www.elsevier.com/locate/ijms

Determination of phosphate position in hexose monosaccharides using an FTICR mass spectrometer: ion/molecule reactions, labeling studies, and dissociation mechanisms

Michael D. Leavell [a], Gary H. Kruppa [b], Julie A. Leary [a,*]

[a] *Department of Chemistry, University of California, Berkeley, CA 94720, USA*
[b] *Sandia National Laboratories, Livermore, CA, USA*

Received 15 April 2002; accepted 3 August 2002

Abstract

Determination of phosphate position in carbohydrates using mass spectrometry is difficult due to the low energy loss of the phosphate either as a neutral or as an ion in MS/MS experiments. A possible solution to this problem is proposed in this work, whereby we use ion/molecule reactions in combination with tandem mass spectrometry to determine the site of phosphorylation on phosphorylated monosaccharides. Singly charged negative ions from phosphorylated monosaccharides are reacted with trimethyl borate in an FTICR MS analyzer cell to produce ion/molecule reaction products with the loss of a neutral methanol molecule. This reaction product likely involves a covalent bond between one of the phosphate oxygen atoms and boron. Derivatization of the phosphate in this manner allows stabilization of the phosphate group under SORI-CID conditions, allowing generation of ions characteristic of the phosphate linkage. Ion structures and dissociation mechanisms explaining these results are presented and discussed. The mechanistic studies suggest that the extra degrees of freedom provided by the 6-linked phosphate allows formation of diagnostic ions in the 6-linked case that are not formed from the 1-linked isomer. The dissociation of the ion/molecule reaction products using infrared multi-photon dissociation (IRMPD) as an activation method was also investigated. While SORI-CID and IRMPD activation yield similar dissociation patterns, the characteristic differences in the product ion spectra between the monosaccharides phosphorylated in the 1- and 6-positions are not observed using IRMPD. (Int J Mass Spectrom 222 (2003) 135–153)

Keywords: Phosphorylated carbohydrates; FTICR MS; Ion/molecule reactions; SORI-CID; IRMPD; Monosaccharide; Phosphate linkage

1. Dedication

In this issue honoring Jack Beauchamp, we are pleased to present our research that involves techniques that Jack either introduced or with which he was an early and influential investigator. Jack's early work involved the use of ion cyclotron resonance (ICR) mass spectrometry to investigate the structure, thermodynamics, and ion/molecule reaction kinetics of organic and organometallic ions, and his contributions in this area have been enormous, as discussed elsewhere in this issue. In this particular study, we show that ion/molecule reactions may be useful to solve a difficult problem in analytical mass spectrometry;

* Corresponding author. E-mail: leary@socrates.berkeley.edu

1387-3806/02/$ – see front matter
PII S1387-3806(02)00986-7

the determination of phosphate linkage position for phosphorylated monosaccharides. With the proliferation of FTICR MS instruments we believe that many new analytical applications of ion/molecule reactions will be found and their use will increase greatly. Jack was also one of the first to investigate the use of IR lasers for the study of structure and dissociation of gas-phase ions using ICR [1]. In this study, we also show that infrared multi-photon dissociation (IRMPD) can be used to easily produce structurally significant product ions from monosaccharides.

2. Introduction

Phosphorylated carbohydrates are ubiquitous in nature and play major roles in the biosynthesis of oligosaccharides and glycolysis [2,3]. Lipooligosaccharides (LOS), a major component of bacteria cell walls, are highly phosphorylated and have been implicated in the virulence of these bacteria [4–6]. In *Haemophilus influenzae*, a Gram-negative pathogen that causes otitis media, meningitis, and upper respiratory infections in children [4,6], the gene *kdkA* has been shown to be essential for the virulence of the organism [6]. This gene encodes the 2-keto-3-deoxy-octulosonic acid (kdo) kinase, which phosphorylates the 4-position of kdo residues present in the LOS of this organism. Since homologs of the *kdkA* gene are present in *Bordetella pertussis*, *Vibrio cholerae*, and other pathogenic bacteria [6], it is likely that phosphorylation is equally important in these bacteria as well.

Phosphorylation has also been shown to be important to the integrity of the cell wall in *H. influenzae* [4]. Mutation of the *htrb* gene results in mutants of *H. influenzae* that have a hypersensitivity to kanamycin, as well as a sensitivity to hydrophobic agents, as compared to the wild type. The LOS of this mutant lacks a phosphate group normally linked to heptose I of the LOS core structure. Since the LOS is a major component of the cell membrane, it is thought that this group plays a central role in the coherence of the cell membrane (i.e., its absence in the mutant strain causes the sensitivities described earlier).

Several studies have been aimed at determining the sites of phosphorylation in proteins using mass spectrometry, as has been recently reviewed by McLachlin and Chait [7]. Phosphopeptide analysis is achieved through several methods including: (1) chemical tagging of phosphorylation sites [8,9], (2) peptide mapping and phosphatase treatment [10], and (3) and various tandem mass spectrometry methods [7] (e.g., post-source decay, precursor ion scan, neutral loss scanning, etc.). Identification of phosphorylation sites is achieved through collision-induced dissociation (CID) of the peptide [11], electron capture dissociation [12], or other dissociation methods [7]. In contrast to proteins, analysis of phosphate position in carbohydrates has not been the focus of many research efforts.

Analysis of phosphate position in carbohydrates is often problematic using mass spectrometry. In the CID analysis of underivatized phosphate-containing oligosaccharides (or peptides/proteins), phosphate cleavage is observed with production of such species as PO_3^-, $H_2PO_4^-$, HPO_3, or H_3PO_4 [7,13]. Thus, either the charge is lost from the oligosaccharide (and the neutral sugar can no longer be analyzed), or the phosphate is lost from the oligosaccharide and an alkoxide results in its former position. In either case, the phosphate position is indeterminate. Early studies used trimethylsilyl derivatization of sugar phosphates followed by GC and GC/MS analysis to determine the phosphorylation site and the stereochemistry of the sugar [14,15]. In a recent study Feurle et al. [13] utilized LC/ESI/MS/MS to structurally characterize phosphorylated carbohydrates using a β-cylcodextrin-bonded stationary phase. Phosphate cleavage is of great concern in the analysis of larger phosphorylated oligomers, where several stages of tandem mass spectrometry are needed to elucidate the structure of the biomolecule, and phosphate loss is enhanced.

In a previous report [16], it was shown that phosphate position could be determined using ion/molecule reactions in combination with tandem mass spectrometry on an FTICR mass spectrometer in the negative ion mode. Ion/molecule reactions between the phosphorylated hexose (HexXP, where X = 1 or 6

indicating the linkage of the phosphate to the monosaccharide) and trimethyl borate (TMB) take place in the FTICR cell. Gas-phase derivatization obviates the need for solution-phase modification, which can result in further sample loss—a major problem for the analysis of compounds isolated in limited quantities from biological systems. Previous studies have shown that TMB reacts with hydrogen-bonded alkoxides [17] as well as phosphorylated amino acids [18] in the gas phase, and is, therefore, a good candidate for investigation. After formation of the ion/molecule reaction product, it is isolated and subjected to SORI-CID, which yields diagnostic ions that are indicative of the phosphate position. Thus, phosphate position may be determined based on the absence or presence of the diagnostic product ions in the MS/MS spectra. In the current study, the mechanism of linkage differentiation is explored using isotopic-labeling data, deoxy analogs, and generational mapping. Further, IRMPD is utilized as a dissociation technique allowing the investigation of different dissociation pathways. Taken together, these data are used to postulate the mechanisms of formation of the diagnostic ion for the Hex6Ps, and further determine the underlying reason why this ion is not observed in the Hex1Ps.

3. Experimental

3.1. Instrumentation

Bruker-Daltonics (Billerica, MA) Apex II FTICR mass spectrometers were used for these studies. They were equipped with 7.0 T superconducting magnets, an Analytica electrospray source (Branford, CT), and a Synrad (Mulkiteo, WA) 25 W IRMPD CO_2 laser. All monosaccharides were analyzed using electrospray ionization (ESI) in the negative ion mode, at a concentration of approximately 30 μM. The solvent system used was 1:1 water/methanol or 1:1 water/acetonitrile with no added acid or base. The ions produced by ESI were accumulated external to the FTICR MS trapping cell [19] in a hexapole ion guide for ∼1 s. After accumulation, the ions were pulsed out of the ion guide and transferred to the FTICR MS analyzer cell by electrostatic ion optics, where they were trapped. Trapping was accomplished by either "sidekick" [20] ion accumulation or gated trapping [21] using a dynamic trapping accessory available for the FTICR MS instrument. It was important to use gated trapping for all of the IRMPD experiments with the sidekick voltage (DEV2 parameter on the Bruker Daltonics instrument) set to 0.0, in order to keep the ions on the center axis of the cylindrical cell, allowing interaction of the ions with the IRMPD laser beam.

Tandem mass spectrometry (MS^n) experiments were performed by isolation of the desired precursor ion by a CHEF [22] isolation sweep, followed by ion activation and dissociation by either SORI-CID [23] or IRMPD [1]. For clean isolations, it was necessary to apply single frequency "cleanup" shots to eject small amounts of product ions formed from the off-resonance excitation of the very fragile precursor ions during the CHEF isolation sweep. For SORI-CID, Ar gas was pulsed into the FTICR MS analyzer cell to raise the pressure in the cell into the low 10^{-6} mbar range, and the ions were then activated 500 Hz off-resonance for 250 ms. The amplitude of the off-resonance irradiation was adjusted to give nearly complete attenuation of the precursor ion signal; this was typically in the range of 1.5–4.5 V_{p-p} (attenuation of 38–50 dB in the system software). After a delay of several seconds to allow pump-down of the collision gas pulse, the product ions were detected under high-resolution conditions. For IRMPD [1] experiments, the IR laser (defocused) was turned on after the ion isolation for 300 ms at a power level of 20–40% of full power (25 W) for 250 ms, corresponding to a power range between 5 and 10 W, and the product ions could immediately be detected under high-resolution conditions.

For MS^n studies on the products of the ion/molecule reactions, TMB was pulsed into the FTICR MS analyzer cell after the ion-trapping event. The TMB reagent was first degassed by several freeze–pump–thaw cycles. The room temperature vapor pressure of the TMB reagent was such that the pulsed valve

could be held open for several seconds if desired and the steady state pressure of the reagent in the analyzer cell was 2×10^{-7} mbar with the valve open. In some cases where the desired product of this reaction gave a weak signal, the signal was enhanced by multiple cycles of external ion accumulation, ion-injection, and reagent gas pulse. The TMB gas pulse was typically between 50 ms and 1 s per cycle.

3.2. Synthesis and labeling studies

Enzymatic synthesis of the non-exchangeable D-labeled analogs or the 3-deoxy glucose-6-phosphates (3-deoxy-Glc6Ps) was accomplished through modification of a previously published procedure [24]. The appropriate glucose derivative (0.75 μmol), ATP (Mg^{2+} salt 0.15 μmol), and 1.11 units of the hexokinase enzyme were mixed in 60 μL of 225 mM ammonium acetate buffer (pH 7.6) and allowed to react while gently rocking for 1 h at 25 °C. Exact mass measurements were performed to characterize each of the enzymatically synthesized compounds. In all cases the error between the measured and exact mass was less than 2 ppm. Labeling of the reducing end with ^{18}O was accomplished by dissolving the monosaccharide sample in ^{18}O-labeled water, followed by heating at 80 °C for 30 min. Similarly, deuterium-labeling of all exchangeable protons was accomplished by heating the monosaccharide sample in D_2O at 80 °C for 30 min. All labeled compounds were diluted in appropriately labeled solvents (D-labeled or ^{18}O) and experiments were performed as noted earlier.

3.3. Chemicals and materials

Hexose phosphates, hexokinase, and ATP were purchased from Sigma Chemical Company (St. Louis, MO). TMB, ^{18}O-labeled water, CD_3OD, and D_2O were purchased from Aldrich Chemical Company (Milwaukee, WI). Isotopically labeled hexoses were purchased from OMICRON Biochemicals (South Bend, IN). All solvents and ammonium acetate were purchased from Fisher and the solvents were of HPLC grade.

4. Results and discussion

4.1. SORI-CID of underivatized hexose phosphates

The hexose phosphates, studied in this investigation are shown in Fig. 1. Both the phosphate position and the stereochemistry of the monosaccharide were varied to determine the applicability of this technique to different structural features. As discussed in Section 2, analysis of phosphate-containing saccharides by mass spectrometry is often problematic as is illustrated in Fig. 2. Fig. 2A shows the SORI-CID spectrum of glucose-1-phosphate (Glc1P), while Fig. 2B shows the SORI-CID spectrum of Glc6P. When subjected to SORI-CID, both glucose phosphate precursor ions (*m*/*z* 259) dissociate through many different dissociation channels, but the most favorable channel is formation of the dihydrogen phosphate ion ($H_2PO_4^-$) which is observed at *m*/*z* 97. Thus, neutral loss of the sugar is the main pathway through which the hexose phosphates dissociate. Several other product ions are also observed in these spectra. Loss of H_2O from the precursor ion is observed at *m*/*z* 241, while loss of H_3PO_4 is observed at *m*/*z* 161. Furthermore, two cross-ring cleavage ions are observed at *m*/*z* 199 and 169, corresponding to loss of $C_2H_4O_2$ and $C_3H_6O_3$, respectively. Three of the ions mentioned earlier (*m*/*z* 241, 199, and 169), still contain phosphate and would normally be considered candidates for further stages of tandem mass spectrometry, to determine phosphate position. However, their low ion current precludes further analysis of these ions by tandem mass spectrometry. Furthermore, the spectra are strikingly similar; therefore, differentiation of the phosphate linkage would not be easily accomplished.

4.2. Ion/molecule reaction of HexXP with TMB

Reaction of the hexose phosphates with TMB yielded two ion/molecule reaction complexes (Fig. 3, Table 1), which are observed at *m*/*z* 331 and 299, corresponding to $[HexXP/B(OMe)_3–MeOH–H]^-$ and $[HexXP/B(OMe)_3–2MeOH–H]^-$, respectively (where

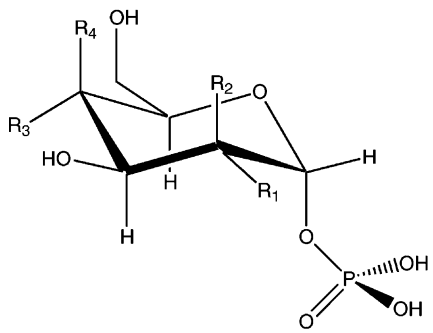

α-D-Hexose-1-Phosphate (Hex1P)

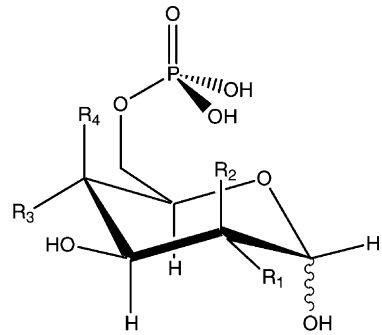

D-Hexose-6-Phosphate (Hex6P)

Structure of the Hexoses Investigated.

	R_1	R_2	R_3	R_4
Glc	-OH	-H	-OH	-H
Gal	-OH	-H	-H	-OH
Man	-H	-OH	-OH	-H

Fig. 1. Structure of the hexose phosphates investigated.

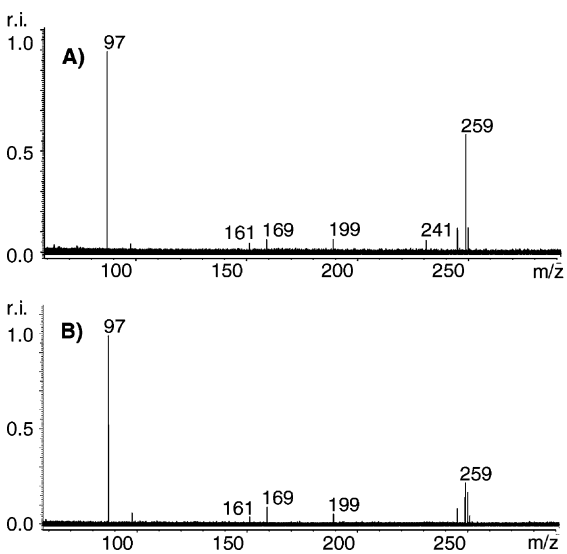

Fig. 2. SORI-CID dissociation of underivatized (A) Glc1P and (B) Glc6P.

Hex = Glc, Gal, or Man and X indicates the phosphate linkage, either 1 or 6). Postulated ion structures are shown in Fig. 4. In all cases it is assumed that the TMB initially adds to the anionic site, followed by elimination of methanol. Each structure is believed to contain a four-membered ring between the boron and phosphorus atoms with bridging-oxygen atoms.

Table 1
Relative abundance of *m/z* 331 and 299 in the reaction of TMB with the HexXPs

Hexose	*m/z* 331 (%)	*m/z* 299 (%)
Glc1P	100	19
Gal1P	100	16
Man1P	100	58
Glc6P	17	100
Gal6P	86	100
Man6P	33	100

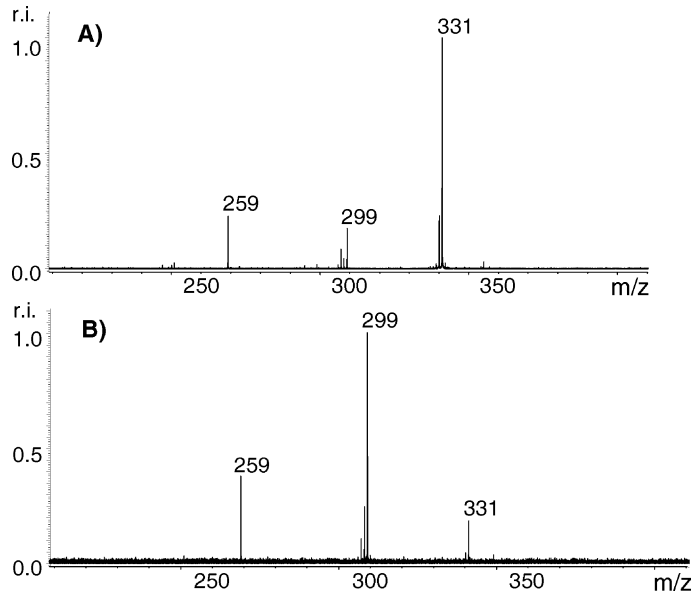

Fig. 3. The ion/molecule reaction between TMB and the (A) Glc1P and (B) Glc6P.

This proposed structural motif is supported by crystal structures of inorganic complexes that show the same four-membered structure [25]. In a previous study [18], Gronert and O'Hair investigated the reaction between TMB with phosphates and their non-covalent complexes. They observed that methanol elimination occurs after the addition of TMB. Further, these losses were consistent with the number of acidic protons available in the systems and these losses are a result of the exothermicity of the addition/elimination reaction. In the study outlined herein, it was generally noticed that the Hex6Ps showed predominant loss of two neutral MeOHs (*m*/*z* 299), while the Hex1Ps showed only one neutral MeOH loss (*m*/*z*

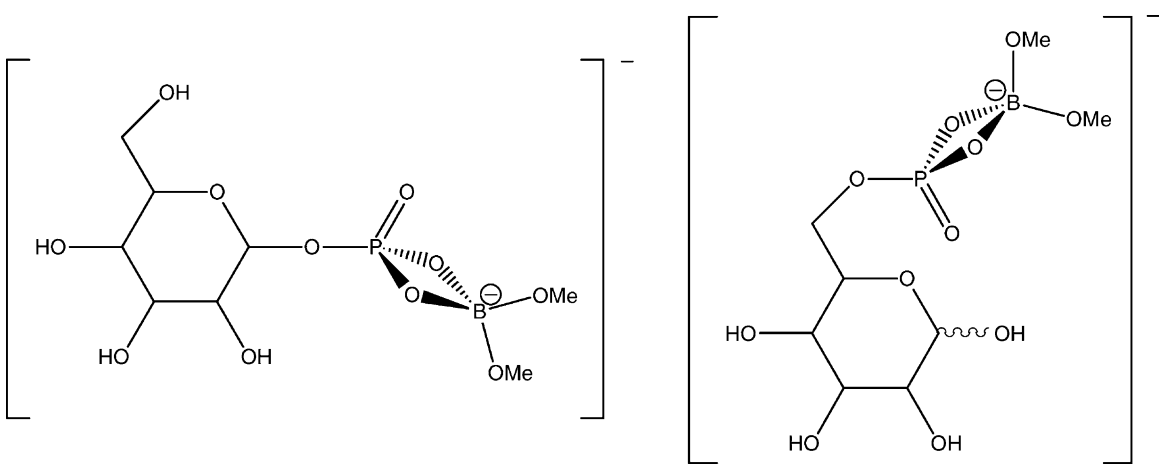

Fig. 4. Proposed structures of the *m*/*z* 331 ion for the Hex1P and the Hex6P.

331, Table 1). This trend has been observed with the 1,2-cyclopentane and cyclohexane diols in CI experiments with protonated TMB, and is thought to be due to the stereochemistry of the adjacent hydroxyl group [26]. In the two HexXP isomers investigated, the ratio of *m/z* 299 and 331 seems to reflect the stereochemistry of the adjacent hydroxyl group (C(4) for Hex6P and C(2) for Hex1P), however, the extra degree of freedom afforded to the phosphate in the Hex6Ps is likely to play a larger role than the stereochemistry of the adjacent hydroxyl group.

4.3. SORI-CID of HexP/TMB derivatives and phosphate linkage determination

Upon isolation and SORI-CID of *m/z* 331, several differences are noted between the derivatized and underivatized hexose phosphates (Figs. 2 and 5, Table 2). In particular, the dihydrogen phosphate ion is no longer the base peak in the SORI-CID spectrum, instead the base peak is observed at *m/z* 299 corresponding to neutral loss of one methanol molecule. Further methanol elimination is also observed at *m/z* 267. It is also interesting to note that the metaphosphate ion (PO_3^-), observed at *m/z* 79, now becomes a dominant product ion in the spectrum, while it was absent in the underivatized case. Cross-ring cleavages normally observed in the underivatized case are no longer observed, except when Gal6P is employed (Table 2). However, the cross-ring cleavage now occurs in combination with loss of one methanol. Given the dramatically different dissociations observed for the ion/molecule reaction products in comparison to the phosphorylated hexoses, it is apparent that addition of TMB allows stabilization of the phosphate group on the sugar. Furthermore, differences in the product ions observed for the different phosphate linkages may be used to determine the phosphate position on these molecules.

Phosphate linkage may be determined based on the absence or presence of diagnostic ions. These ions are observed at *m/z* 249 and 123 for the Hex6Ps but are

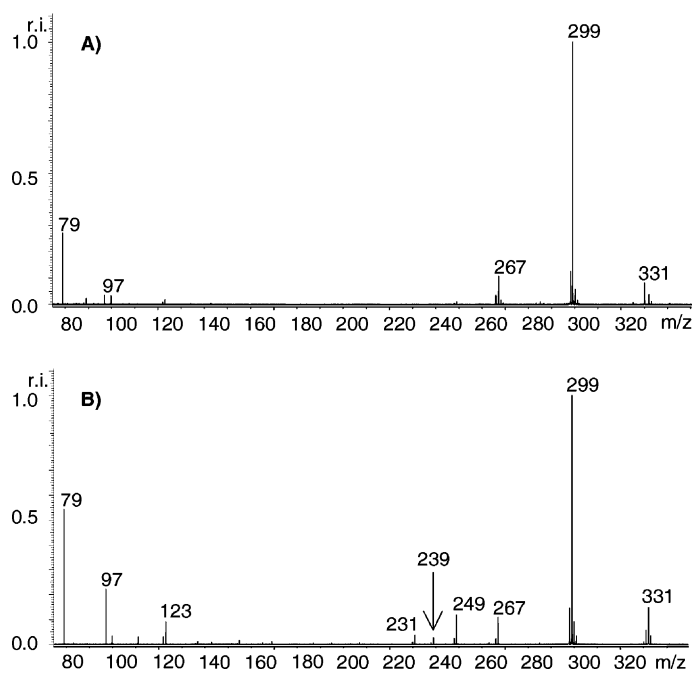

Fig. 5. SORI-CID dissociation of *m/z* 331 (MS^2 331→) for the derivatized hexose phosphates: (A) $[Glc1P/B(OMe)_3–MeOH–H]^-$ and (B) $[Glc6P/B(OMe)_3–MeOH–H]^-$.

Table 2
Product ions observed[a] when [HexP/B(OMe)$_3$–MeOH–H]$^-$ (*m*/*z* 331) is subjected to SORI-CID

	−MeOH *m*/*z* 299	−2MeOH *m*/*z* 267	−2MeOH/H_2O *m*/*z* 249	−MeOH/$C_2H_4O_2$ *m*/*z* 239	−2MeOH/2H_2O *m*/*z* 231	−2MeOH/$C_2H_4O_2$ *m*/*z* 207	HPO_5B^- *m*/*z* 123	$H_2PO_4^-$ *m*/*z* 97	PO_3^- *m*/*z* 79
Glc1P	X	X						X	X
Glc6P	X	X	X	X	X		X	X	X
Gal1P	X	X						X	X
Gal6P	X	X	X			X	X	X	X
Man1P	X	X						X	X
Man6P	X	X	X				X	X	X

[a] Product ions are considered present if their relative intensity is 2% or greater.

absent in the SORI-CID spectra of the Hex1Ps. The ion at *m/z* 249 corresponds to loss of 2MeOH/H_2O from the precursor ion (*m/z* 331), while *m/z* 123 corresponds to a molecular formula of $HPO_5{}^{11}B^-$. Investigation of the *m/z* 249 ion is hampered by the lack of commercially available compounds that are ^{18}O-labeled. Instead, labeling studies were undertaken to determine the origin and possible dissociation mechanisms of the *m/z* 123 ion described as follows.

4.4. Labeling data of the $[Hex6P/B(OMe)_3–MeOH–H]^-$ complex

Several experiments were undertaken to probe the mechanisms of formation for the *m/z* 123 ion. These included isotopic-labeling studies, SORI-CID of deoxy derivatives, and generational mapping experiments. The results of the isotopic-labeling and deoxy analog studies are summarized in Table 3. In total three types of labeling studies were used to probe the mechanism of dissociation. These include: (1) deuterium exchange of all exchangeable protons, (2) deuterium-labeling of selected non-exchangeable protons, and (3) ^{18}O-labeling of the reducing end oxygen.

Upon deuterium exchange of all exchangeable protons on Glc6P, the fully exchanged ion was isolated and subjected to SORI-CID. Following SORI-CID, spectra resulting from the fully-exchanged and the undeuterated compounds were compared. In the fully-exchanged case, three isotope peaks were observed at *m/z* 122, 123, and 124. SORI-CID of the unlabeled Glc6P yielded only *m/z* 122 and 123. The fact that both *m/z* 122 and 124 were observed in the fully exchanged Glc6P suggests that both exchangeable and non-exchangeable protons are incorporated into the diagnostic ion.

Table 3
Results of labeling studies when *m/z* 331 is subjected to SORI-CID

	m/z 122	*m/z* 123	*m/z* 124	*m/z* 125
(A) Deuterium-labeling of non-exchangeable sites				
Unlabeled	X	X		
Glc[1-D]6P	X	X		
Glc[2-D]6P	X	X	X	
Glc[5-D]6P	X	X	X	
Glc[6,6-D_2]6P	X	X		
(B) Deoxy-hexose-6-phosphates				
2-Deoxy-Glc6P		Yes		n/a
3-Deoxy-Glc6P		No		n/a
2-Deoxy-Glc[1-^{18}O]6P		Yes		No

To investigate the origin of the non-exchangeable protons, several Glc6P analogs were investigated, where selected non-exchangeable protons were labeled with deuterium. These included: glucose[1-D]-6-phosphate (Glc[1-D]6P), Glc[2-D]6P, Glc[5-D]6P, and Glc[6,6-D_2]6P (these are the only D-labeled analogs available commercially). The results of these studies are summarized in Table 3 (A). As was discussed earlier in unlabeled Glc6P, only two isotope peaks are observed, *m/z* 122 and 123, which indicates that deuterium is not present in this isotope packet. This trend is observed for the Glc[1-D]6P and the Glc-[6,6-D_2]6P analogs. However, when the Glc[2-D]6P and the Glc[5-D]6P analogs are employed, the isotope packet also included a peak at *m/z* 124. This indicates that a non-exchangeable proton is present in the diagnostic ion. From these results it is apparent that non-exchangeable protons from the C(2) and C(5) carbons are incorporated into the *m/z* 123 ion. From the deuterium-labeling experiments (both exchangeable and non-exchangeable), it is clear that there are at least three mechanisms forming the diagnostic ion.

With all possible deuterium-labeling information in hand, focus turned to determining the origin of the five oxygen atoms contained within *m/z* 123. ^{18}O-Labeling of the reducing end oxygen (C(1)–OH) allowed for investigation of whether it was included in the diagnostic ion, and thus was transferred during the dissociation mechanism. Upon ^{18}O-labeling of the reducing end oxygen, isolation and SORI-CID, it was found that both the *m/z* 123 and 125 ions were observed. Thus, ^{18}O-incorporation occurs, and the C(1)–OH bond must be broken during the formation of the diagnostic ion. It must also be noted, however, that the reducing end oxygen is not the only oxygen atom incorporated into the *m/z* 123 ion. This fact is evidenced by observation of the *m/z* 123 isotope, which corresponds to inclusion of ^{16}O, from another carbohydrate-bound

hydroxyl group. Unfortunately, other ^{18}O-labeled analogs are not available commercially, therefore, the other carbohydrate-bound oxygen atoms contained within the diagnostic ion can only be postulated.

In order to determine which hydroxyl groups were directly involved in diagnostic ion formation, the dissociation of two deoxy analogs were investigated; the 2-deoxy-Glc6P and the 3-deoxy-Glc6P analogs. Upon SORI-CID, *m/z* 123 is observed for the 2-deoxy-Glc6P analog (Table 3, B), however, it does not form in the 3-deoxy analog. Thus, the C(3)–OH is required for formation of the *m/z* 123 ion. One further experiment was performed with the 2-deoxy-Glc6P analog. Since this compound was available commercially (and did not have to be synthesized enzymatically), it was easily ^{18}O-labeled at the reducing end. Examination of the SORI-CID spectra of this derivative, shows that the C(2)–OH must be present to allow the ^{18}O-label to be incorporated into the diagnostic ion. Thus, through labeling studies several important pieces of information regarding the dissociation mechanism have been determined. These are: (1) both non-exchangeable (specifically the C(2)–H and the C(5)–H protons) and exchangeable protons are incorporated into the diagnostic ion, (2) the C(3)–OH must be present for the diagnostic ion to form, and (3) the C(2)–OH must be present for the ^{18}O-label at the reducing end oxygen to be incorporated into the *m/z* 123 diagnostic ion.

4.5. Generational mapping

With the MS^2 and labeling data in hand, it was decided to investigate the differences in dissociation between the *m/z* 331 ion to that of the *m/z* 299 ion generated in the MS^3 (331 → 299 →) experiment (Table 4, Fig. 6). Exploration of the dissociation of this ion could yield information regarding the mechanism of diagnostic ion formation, or perhaps more structural information of the ion/molecule reaction complexes. Several features of the MS^3 spectra are worth noting. As was observed in SORI-CID of *m/z* 331, neutral losses of MeOH and H_2O dominate the spectra. Furthermore, the Hex6Ps show a larger abundance of product ions, again illustrating the low dissociation thresholds present in the Hex6Ps, that are not found in the Hex1Ps. Also, cross-ring cleavage of the monosaccharide ring is observed both with (*m/z* 207) and without (*m/z* 239) neutral MeOH loss. However, the most intriguing result of these experiments is the presence of *m/z* 123 for both the Hex1Ps and the Hex6Ps. Furthermore, SORI-CID of the *m/z* 267 ion (MS^4 experiment, 331 → 299 → 267 → , data not shown) yielded the *m/z* 123 ion as well. Information from the generational mapping and the labeling experiments were used to elucidate the mechanism of formation for *m/z* 123.

4.6. Dissociation mechanisms

Using the data generated from the labeling experiments, deoxy studies, and the generational mapping experiments, three mechanisms of *m/z* 123 ion formation are proposed. Scheme 1 illustrates the proposed dissociation mechanism that highlights the requirements determined by the D-exchange experiments, the deoxy studies and the ^{18}O-labeling data. Upon SORI-CID of the *m/z* 331 ion (1a), elimination of

Table 4
Product ions generated[a] from SORI-CID of the parent ion $[HexP/B(OMe)_3–2MeOH–H]^-$ (*m/z* 331 → 299 →)

	−MeOH *m/z* 267	$-MeOH/H_2O$ *m/z* 249	$-C_2H_4O_2$ *m/z* 239	$-MeOH/2H_2O$ *m/z* 231	$-MeOH/C_2H_4O_2$ *m/z* 207	$-2MeOH/2H_2O$ *m/z* 195	HPO_5B^- *m/z* 123	$H_2PO_4^-$ *m/z* 97	PO_3^- *m/z* 79
Glc1P	X	X	X	X		X	X	X	X
Gal1P	X	X					X	X	X
Man1P	X	X		X		X	X	X	X
Glc6P	X	X	X	X	X	X	X	X	X
Gal6P	X	X		X	X		X	X	X
Man6P	X	X	X	X		X	X	X	X

[a] A 2% relative abundance criterion is used to determine the absence or presence of an ion.

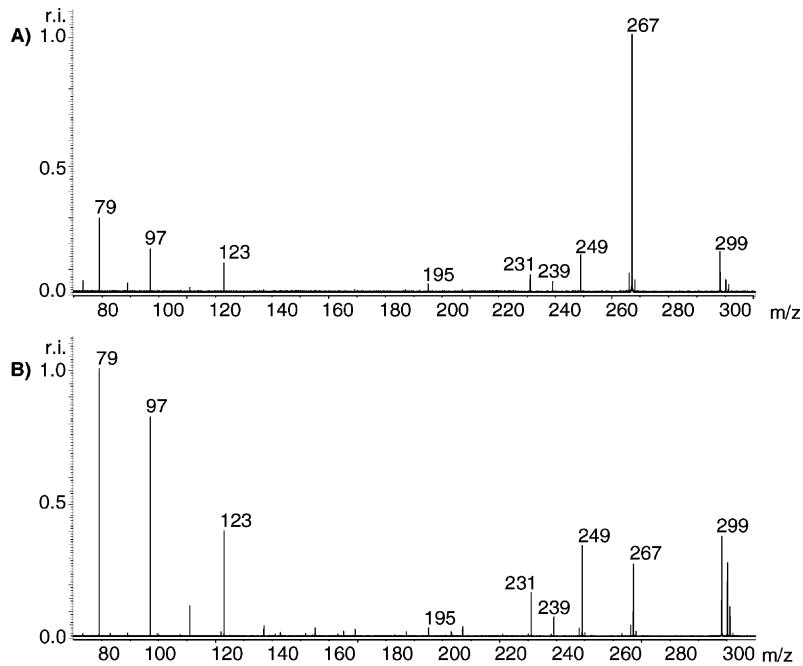

Fig. 6. SORI-CID dissociation of *m/z* 299 (MS^3 331→299→) for generational mapping: (A) $[Glc1P/B(OMe)_3–2MeOH–H]^-$ and (B) $[Glc6P/B(OMe)_3–2MeOH–H]^-$.

MeOH occurs through deprotonation of the C(1)–OH, by a methoxy group bound to the boron-center. Following neutral loss of MeOH, and proton transfer, an alkoxide is generated at C(3) (1b). Both the proton transfer and alkoxide generation at C(3) are supported by the deoxy-labeling studies, which show that the C(3)–OH is critical in the mechanism of *m/z* 123 ion formation (Table 3, B). Further, the ^{18}O-labeled 2-deoxy-Glc6P analog showed that the ^{18}O-label was not included in the diagnostic ion upon SORI-CID. Thus, the C(2)–OH is involved in the proton transfer mechanism that allows alkoxide generation at C(3). Cross-ring cleavage is initiated by the C(3) alkoxide, resulting in double bond formation between C(1) and C(2) and ^{18}O-transfer to the B-center. This step is required by the ^{18}O-labeling experiment, regenerating a four-coordinate B-center (1c). Loss of a second MeOH is postulated to occur through deprotonation of the ^{18}O-labeled hydroxyl group bound to the boron-center, yielding *m/z* 267 (1d). From the generational mapping experiments, it is known that *m/z* 123 can be formed from *m/z* 299 and 267. Thus, in all mechanisms we propose sequential MeOH loss. Following ring opening of the four-membered ring between the B- and P-atoms (1d), an oxyanion site is formed on the phosphate moiety. Finally, deprotonation of the C(4)–OH (1e) through an eight-membered intermediate by the oxyanion site yields the *m/z* 123 ion (1f) with simultaneous loss of glyoxal (OHCCHO) and $C_2H_6O_2$.

The ion at *m/z* 123 can also be generated via another mechanism in the 2-deoxy analog as shown in Scheme 2. In this mechanism, initial deprotonation occurs at C(4) allowing MeOH loss (2a), followed by proton transfer and alkoxide generation at C(3) (2b). In order for hydroxyl transfer to occur to the B-atom, rotation around the C5–C6 bond must occur to position the B-atom in proximity to the C(1)–OH (2b). However, for the diagnostic ion to form, deprotonation at the C(4)–OH must occur which requires another rotation around the C5–C6 bond (2e). Excessive rotation of this nature would hinder formation of the *m/z* 123 ion due to entropic constraints, and thus is

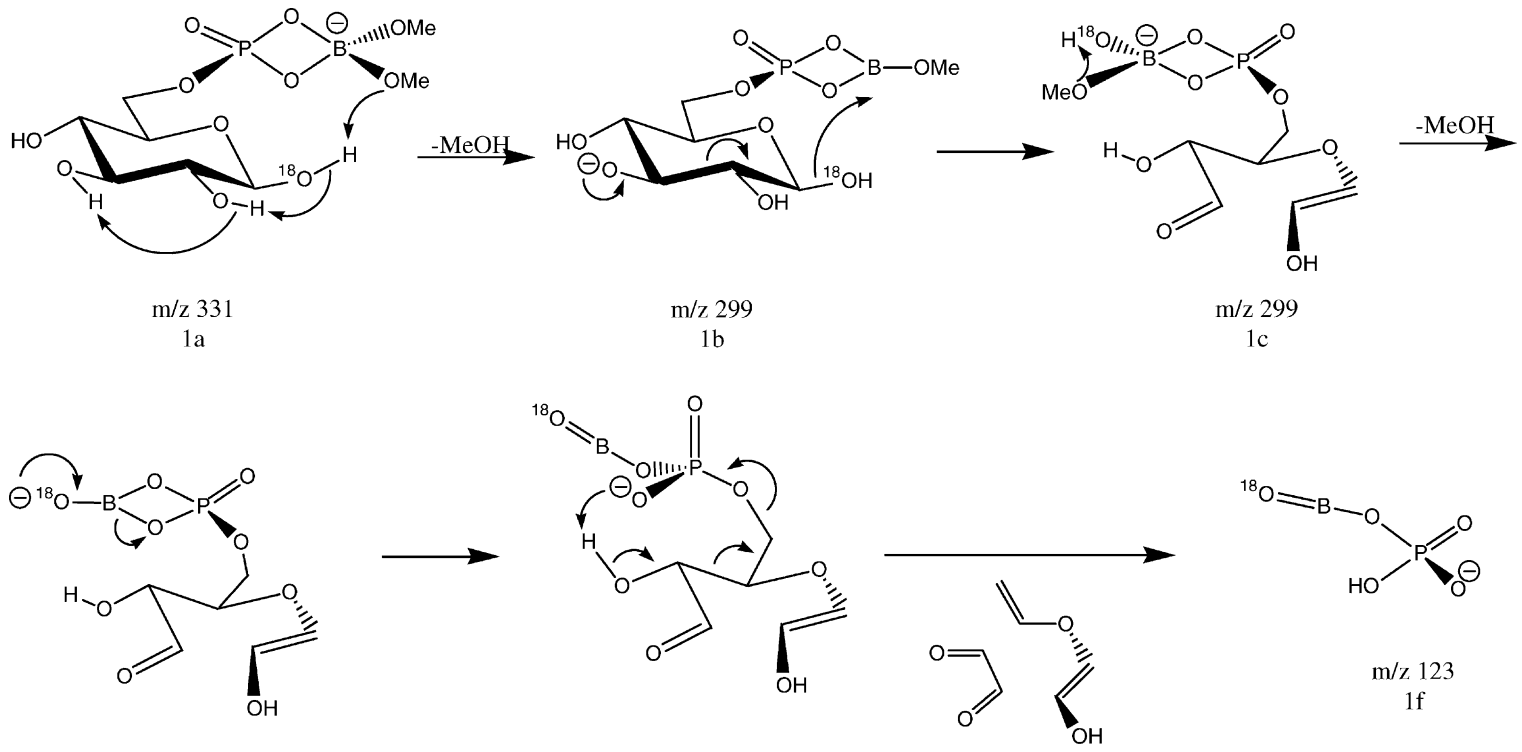
-MeOH
-MeOH
m/z 331
1a
m/z 299
1b
m/z 299
1c
m/z 267
1d
m/z 267
1e
m/z 123
1f

Scheme 1.

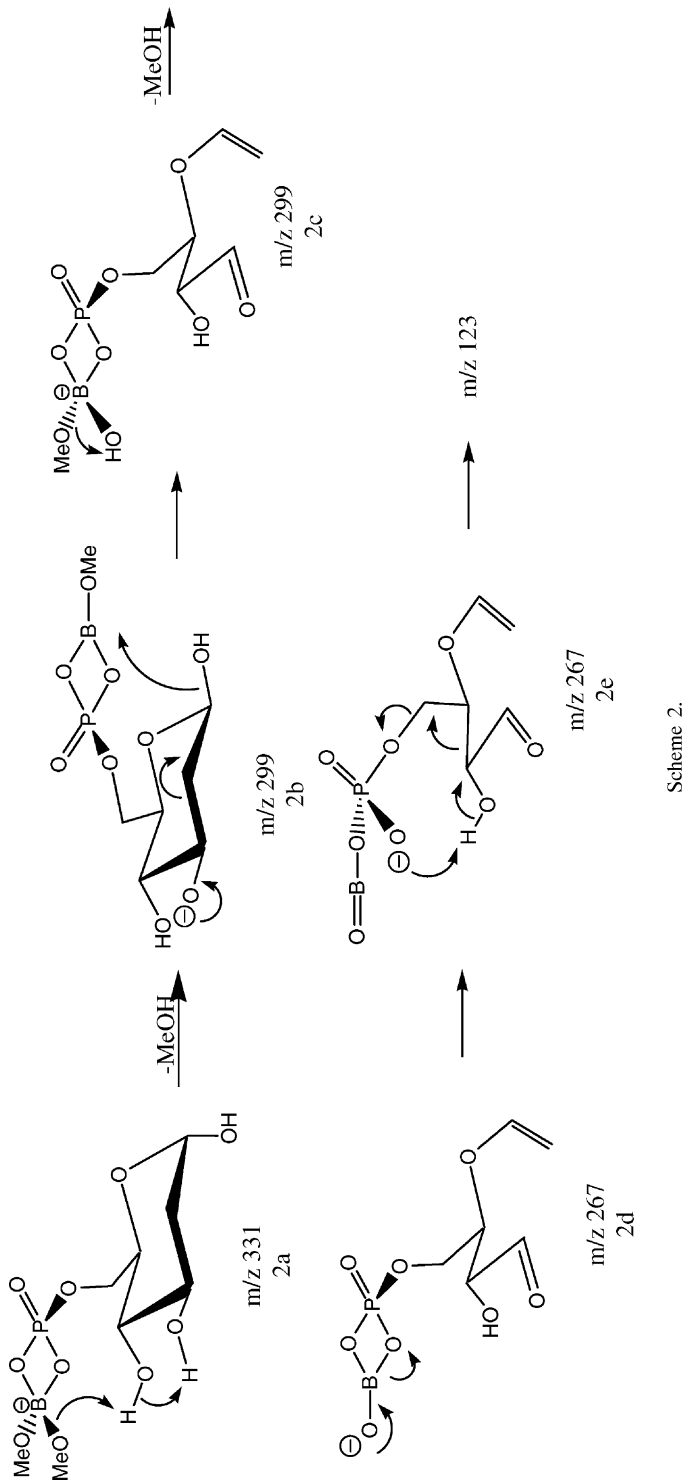

Scheme 2.

postulated to occur *only* when the 2-deoxy analog is employed.

Scheme 3 illustrates the proposed dissociation mechanism that highlights the requirements determined by the deoxy studies and the non-exchangeable deuterium-labeling experiment using the Glc[5-D]6P analog. The initial loss of methanol is postulated to occur through deprotonation of the C(4)–OH by a methoxy group bound to the B-center (3a). Following proton transfer and generation of an alkoxide at C(2), the monosaccharide ring opens, and the C(4)-hydroxyl group is transferred to the B-atom (3b). Again, the presence of the C(3)-hydroxyl is required by this mechanism, as was found in the deoxy studies. Given the fact that hydroxyl group transfer was observed in the ^{18}O-labeled analog in Scheme 1, we postulate that this can also occur at the C(4)-hydroxyl, given the close spatial proximity of this hydroxyl group to the boron–phosphate moiety. Formation of *m*/*z* 267 is again postulated to occur through deprotonation of the hydroxyl bound to the boron-center (3c). Following the opening of the four-membered ring (3d), deprotonation of the C(4) carbon-center occurs through a six-membered intermediate (3e). This deprotonation step is confirmed through SORI-CID of the Glc[5-D]6P analog described earlier, yielding a neutral loss of $C_6H_9O_4$ and formation of the *m*/*z* 123 ion.

Scheme 4 shows the proposed mechanism for *m*/*z* 123 ion formation from Glc1P. Like the two previous mechanisms for the Hex6Ps, generation of *m*/*z* 299 from *m*/*z* 331 might occur through loss of MeOH through deprotonation of a sugar ring hydroxyl (C(2)–OH) by a methoxy group bound to the B-center (4a). Proton transfer allows alkoxide generation at C(4) and following ring opening the C(2)-hydroxyl is transferred to the B-center (4b). Progression from *m*/*z* 299 to 267 again occurs via proton transfer from the hydroxyl group bound to the B-center yielding a MeOH loss (4c). This is followed by four-membered ring opening, and an oxyanion is generated on the phosphate moiety (4d). Up until this point the energies of the proposed dissociation mechanisms for both the Hex6Ps and the Hex1Ps are virtually identical. However, it is the progression from structure (4e) to (4f) that we propose causes the differentiation of the Hex1Ps from the Hex6Ps to occur. In this step, deprotonation of the C(3)–OH by the oxyanion on the phosphate moiety is hindered by the ring strain needed to form this "*trans*-cyclooctene" equivalent. Using ring strain in cycloalkanes and cycloalkenes as a guide, this eight-membered intermediate with a *trans*-double bond should be approximately 5 kcal/mol higher in energy than the corresponding cyclooctane (1e), and approximately 15 kcal/mol higher in energy than the corresponding cyclohexane (3e) [27]. Thus, we propose that due to the extra energy between the transition states of these mechanisms, we observe the diagnostic ion in the MS^2 spectra of the Hex6Ps, while it is absent from the Hex1Ps.

4.7. IRMPD of HexP/TMB derivatives

IRMPD is a technique that was first developed to characterize the structure and dissociation of low *m*/*z* ions studied by FTICR MS [1]. A number of groups have shown more recently that IRMPD is applicable to a wide range of biomolecules [28]. In particular, a recent study using FTICR MS by Marshall and coworkers [29] shows that IRMPD is a useful tool for the structural elucidation of naturally occurring oligosaccharides. When subjected to SORI-CID many natural products, including oligosaccharides, undergo multiple facile losses of H_2O and MeOH before cross-ring or glycosidic cleavages occur that can be used to determine linkage and topology of the oligosaccharide, respectively. Since SORI-CID is a resonant technique, product ions produced by SORI-CID do not undergo further activation and will not dissociate further unless they receive sufficient activation before undergoing the initial dissociation. Thus with SORI-CID of large oligosaccharides, several stages of MS/MS are required to produce structurally significant product ions. In contrast, with IRMPD, product ions that are formed initially will remain in the IR laser beam path and will continue to undergo activation and dissociation as long as the laser beam is left on. Thus, product ions formed by small neutral losses will continue

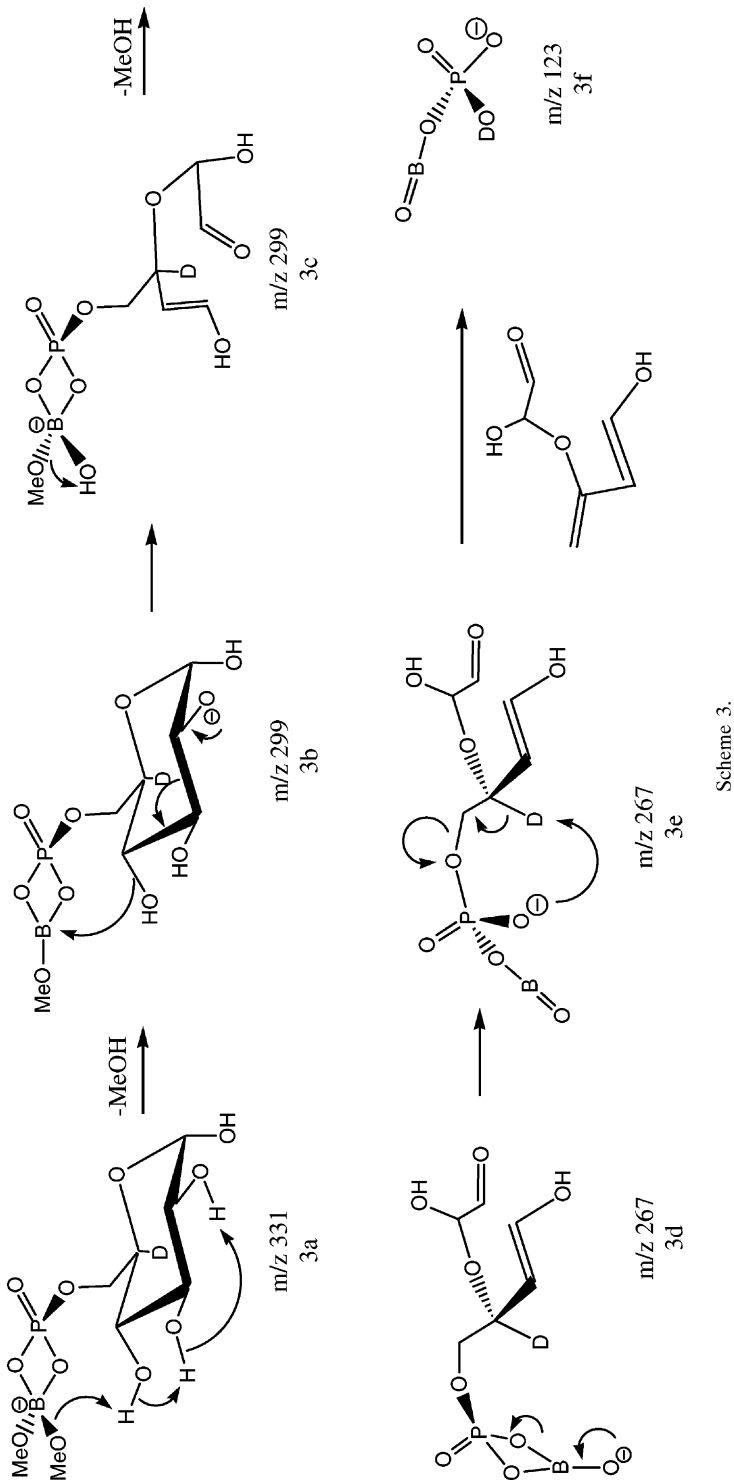

Scheme 3.

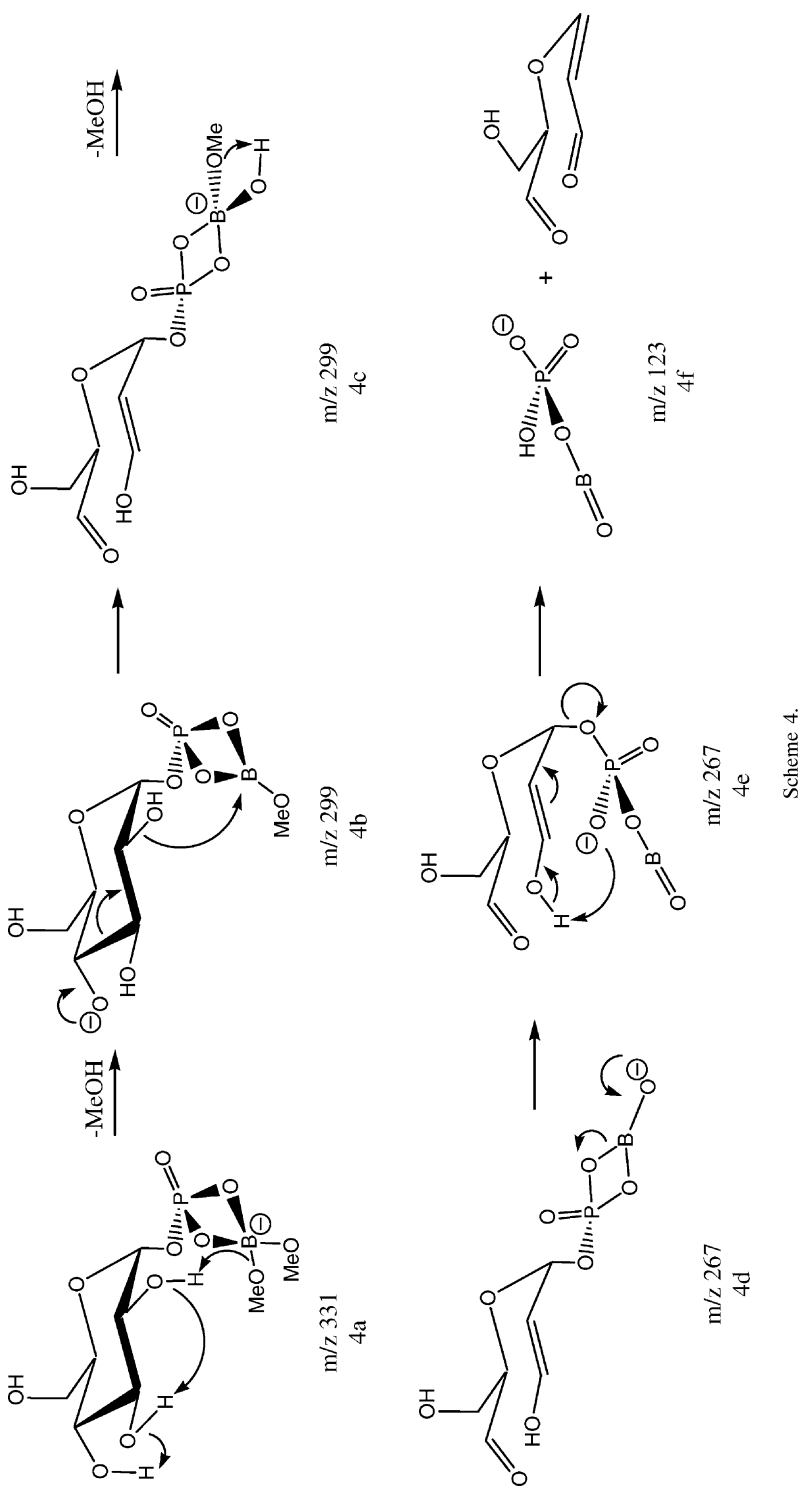
-MeOH
-MeOH
m/z 331
4a
m/z 299
4b
m/z 299
4c
m/z 267
4d
m/z 267
4e
m/z 123
4f

Scheme 4.

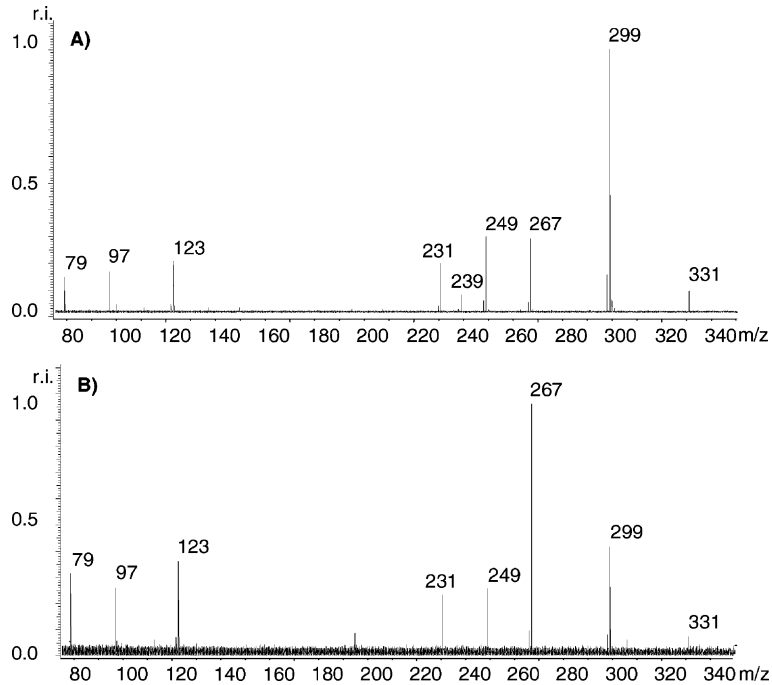

Fig. 7. IRMPD dissociation of *m*/*z* 331 (MS^2 331→) for the derivatized hexose phosphates: (A) [Glc1P/$B(OMe)_3$–MeOH–H]$^-$ and (B) [Glc6P/$B(OMe)_3$–MeOH–H]$^-$. The signal-to-noise in Glc6P is low due to the poor yield of *m*/*z* 331 in the initial ion/molecule reaction.

to dissociate to give structurally informative ions, which would be extremely useful in the case of larger oligosaccharides [29]. Given this significant difference between SORI-CID and IRMPD, it was decided to explore IRMPD of the monomers to determine what, if any, differences might be observed between the two techniques with small molecules. Fig. 7A and B show the IRMPD dissociation spectra of *m*/*z* 331 isolated from the reaction of TMB with Glc1P and Glc6P, respectively, at 30% of full laser power. The lower signal-to-noise (*S*/*N*) in the case of the Glc6P isomer is due to the low relative abundance of the *m*/*z* 331 precursor ion formed in the initial ion/molecule reaction (see Table 1). The ions formed by IRMPD are the same as those seen by SORI-CID MS/MS and on *m*/*z* 331 (Table 2) or on *m*/*z* 299 (Table 4). Additionally the IRMPD experiments produced the *m*/*z* 123 ion for both the Glc1P and Glc6P ions. From Table 2, this is the characteristic ion that allows the linkage position of the phosphate moiety to be determined by SORI-CID MS/MS as it appears only in the spectra of the monosaccharides with the phosphate linked in the 6-position. Although no characteristically different ions are observed between the IRMPD MS/MS spectra of the monomeric isomers studied, the fact remains that this latter technique will become quite important as we implement the ion/molecule reaction method on larger oligomers. The impact of IRMPD on these intermediate product ions is apparent from the observation that by using a shorter irradiation time, it is possible to quantitatively convert the *m*/*z* 331 ion to the *m*/*z* 299 ion. This is further supported by the observation that using lower laser power and shorter irradiation time, it is possible to quantitatively convert the *m*/*z* 331 ion to the *m*/*z* 299 ion by IRMPD. Thus, while IRMPD does not give structurally significant product ions from the monosaccharides studied, it will likely do so for larger oligomers

using the ion/molecule reaction presented in this study.

5. Conclusions

Ion/molecule reactions between TMB and the hexose phosphates have been shown to form ion/molecule reaction complexes with the loss of one or two molecules of neutral methanol. Isolation and dissociation of this species corresponding to one methanol loss (*m*/*z* 331) using SORI-CID yields product ion spectra that show characteristic differences that can be used to distinguish the Hex1Ps from the Hex6Ps. Mechanisms based on SORI-CID studies of labeled (deuterium and ^{18}O) and deoxy derivatives of Glc6P have been proposed. These mechanisms suggest that the difference in product ion intensities between the Hex1Ps and Hex6Ps is due to a difference in ring strain energy in one of the intermediates that is involved in the formation of the characteristic ion at *m*/*z* 123. The Hex1Ps do form this ion with further SORI-CID activation of the *m*/*z* 299 product ion in an MS^3 experiment. This observation explains the production of the *m*/*z* 123 ion in the IRMPD-activated MS^2 spectra of the Hex1Ps, since the product ions may be further activated after their initial dissociation. This is because the ions remain in the IR laser beam path, and this further activation results in the formation of *m*/*z* 123 by IRMPD for the Hex1Ps. This observation is important, as it implies that the SORI-CID results in this study would only be reproduced on mass spectrometers that use low energy, resonant excitation. In triple quadrupoles or quadrupole ion-trap instruments with broadband RF excitation for MS^2, product ions initially produced by the lowest energy dissociation pathways may be further activated by more collisions.

The present study also shows that low energy resonant excitation of precursor ions used in SORI-CID, when combined with ion/molecule reactions can yield product ion relative abundances that are sensitive to small differences in ion structure. Current studies are focused on determining other possible neutral ion/molecule reagents, as well as extensions of this work to phosphorylated oligosaccharides.

Acknowledgements

JAL and MDL gratefully acknowledge NIH Grant No. GM-47356 for funding. GHK acknowledges funding from the Laboratory Directed Research and Development Program at Sandia National Laboratories, which is a multiprogram laboratory operated by Sandia Corporation, a Lockheed Martin Company for the United States Department of Energy under contract DE-AC04-94AL85000. The authors would also like to thank Professor Scott Gronert (San Francisco State University) for his advice and assistance on this project.

References

[1] R.L. Woodin, D.S. Bomse, J.L. Beauchamp, J. Am. Chem. Soc. 100 (1978) 3248.
[2] T. Marquardt, H. Freeze, Biol. Chem. 382 (2001) 161.
[3] D.V. Voet, J.G. Voet, Biochemistry, Wiley, New York, 1990, p. 425.
[4] N.G. Lee, M.G. Sunshine, J.J. Engstrom, B.W. Gibson, M.A. Apicella, J. Biol Chem. 270 (1995) 27151.
[5] J. Lehmann, Carbohydrates: Structure and Biology, Thieme Verlag, New York, 1998, p. 57.
[6] K.A. White, S. Lin, R.J. Cotter, C.R.H. Raetz, J. Biol. Chem. 274 (1999) 31391.
[7] D.T. McLachlin, B.T. Chait, Curr. Opin. Chem. Biol. 5 (2001) 591.
[8] H. Zhou, J.D. Watts, R. Aebersold, Nat. Biotechnol. 19 (2001) 375.
[9] Y. Oda, T. Nagasu, B.T. Chait, Nat. Biotechnol. 19 (2001) 379.
[10] X. Zhang, C.J. Herring, P.R. Romano, J. Szczepanowska, H. Brzeska, A.G. Hinnebusch, J. Qin, Anal. Chem. 70 (1998) 2050.
[11] R.S. Annan, M.J. Huddleston, R. Verma, R.J. Deshaies, S.A. Carr, Anal. Chem. 73 (2001) 393.
[12] A. Stensballe, O.N. Jensen, J.V. Olsen, K.F. Haselmann, R.A. Zubarev, Rapid Commun. Mass Spectrom. 14 (2000) 1793.
[13] J. Feurle, H. Jomaa, M. Wilhelm, B. Gutsche, M. Herderich, J. Chromatogr. A 803 (1998) 111.
[14] M. Zinbo, W.R. Sherman, J. Am. Chem. Soc. 92 (1970) 2105.
[15] D.J. Harvey, M.G. Horning, J. Chromatogr. 76 (1973) 51.
[16] M.D. Leavell, G.H. Kruppa, J.A. Leary, Anal. Chem. 74 (2002) 2608.

[17] H. van der Wel, N.M.M. Nibbering, J.C. Sheldon, R.N. Hayes, J.H. Bowie, J. Am. Chem. Soc. 109 (1987) 5823.
[18] S. Gronert, R.A.J. O'Hair, J. Am. Soc. Mass Spectrom. 13 (2002) 1088.
[19] M.W. Senko, C.L. Hendrickson, M.R. Emmett, S.D.H. Shi, A.G. Marshall, J. Am. Soc. Mass Spectrom. 8 (1997) 970.
[20] P. Caravatti, U.S. Patent No. 4,924,089 (1990).
[21] J.M. Alford, P.E. Williams, D.J. Trevor, R.E. Smalley, Int. J. Mass Spectrom. Ion Processes 72 (1986) 33.
[22] L.J. de Konig, N.M.M. Nibbering, S.L. van Orden, F.H. Laukien, J. Mass Spectrom. Ion Processes 165 (1997) 209.
[23] J.W. Gauthier, T.R. Trautman, D.B. Jacobson, Anal. Chim. Acta 246 (1991) 211.
[24] R. Golbik, M. Naumann, A. Otto, E.-C. Mueller, J. Behlke, R. Reuter, G. Huebner, T.M. Kriegel, Biochemistry 40 (2001) 1083.
[25] R. Kniep, I. Boy, H. Engelhardt, Z. Anorg. Allg. Chem. 625 (1999) 1512.
[26] J.S. Splitter, F. Tureček, Applications of Mass Spectrometry to Organic Stereochemistry, VCH, New York, 1994, p. 435.
[27] T.H. Lowry, K.S. Richardsen, Mechanism and Theory in Organic Chemistry, Harper Collins, New York, 1987, p. 165.
[28] D.P. Little, J.P. Speir, M.W. Senko, P.B. Oconnor, F.W. McLafferty, Anal. Chem. 66 (1994) 2809.
[29] S.D.H. Shi, C.L. Hendrickson, A.G. Marshall, M.M. Siegel, F.M. Kong, G.T. Carter, J. Am Soc. Mass Spectrom. 10 (1999) 1285.